# $^1$H-NMR and photo-CIDNP spectroscopies show a possible role for Trp$^{23}$ and Phe$^{31}$ in nucleic acid binding by P2 ribonuclease from the archaeon *Sulfolobus solfataricus*

Roberto Consonni[a,*], Rita Limiroli[b], Henriette Molinari[c], Paola Fusi[d], Margareth Grisa[d], Marco Vanoni[d], Paolo Tortora[d]

[a]*Istituto di Chimica delle Macromolecole, Lab. NMR, CNR Milano, Via Ampere 56, I-20131 Milano, Italy*
[b]*Istituto Sperimentale per l'Elaiotecnica, Pescara, c/o Istituto di Chimica delle Macromolecole, Lab. NMR, CNR, Via Ampere 56, I-20131 Milano, Italy*
[c]*Istituto Policattedra Università di Verona, Strada Le Grazie, 37134 Verona, Italy*
[d]*Dipartimento di Fisiologia e Biochimica Generali, Università di Milano, Via Celoria 26, I-20133 Milano, Italy*

Received 5 January 1995; revised version received 3 August 1995

**Abstract** **Investigations were performed on recombinant ribonuclease P2 from *Sulfolobus solfataricus*, previously cloned and expressed in *Escherichia coli* [Fusi, P., Grisa, M., Mombelli, E., Consonni, R., Tortora, P. and Vanoni, M. (1995) Gene 154, 99–103]. NMR and photo-CIDNP spectroscopies showed that the enzyme possesses an aromatic cluster constisting of Phe$^5$, Tyr$^7$, Phe$^{31}$ and Tyr$^{33}$ while Trp$^{23}$ is fully exposed to solvent. Phe$^{31}$, Tyr$^{33}$ and Trp$^{23}$ are located within a triple stranded anti-parallel β-sheet, each one being part of an amino acid stretch matching consensus sequences for RNA binding. Phe$^{31}$ and Trp$^{23}$ are exposed to and specifically interact with a flavin dye used as a model ligand, with a topology reminiscent of that found in several eubacterial and eukariotic RNA-binding proteins.**

*Key words:* Archaebacteria; RNA recognition motif; P2; NMR; Photo-CIDNP; *Sulfolobus solfataricus*

## 1. Introduction

In recent years, knowledge of physiological roles and diversity of RNases has remarkably expanded. These enzymes not only sustain non-specific RNA cleavage, but also a variety of other reactions, such as trimming, splicing, addition and modification reactions of RNA molecules [1,2]. However, little is known about archaebacterial RNases. Only two RNase Ps have been identified and characterized until recently, one from *Sulfolobus solfataricus* and another from *Haloferax volcanii* [3]. Thus, we searched for RNases from the thermoacidophilic archaebacterium *S. solfataricus*, and isolated three such enzymes, referred to as P1, P2 and P3 [4]. Extensive characterization of P2 showed that this enzyme cleaves RNA with a narrow substrate specificity and releases 3′-phosphooligonucleotides. Complete primary structure [4] showed that the molecule consists of 62 amino acids, is devoid of any cysteine and histidine, and is closely related to a class of small proteins previously isolated from *S. acidocaldarius* and *S. solfataricus*, and identified as DNA-binding proteins on the basis of their capacity to bind DNA aspecifically [5–7]. Particularly, P2 was identical to the protein previously found in *S. solfataricus* and referred to as Sso7d [7], except for the replacement of Glu$^{13}$ by Gln$^{13}$, and the lack of one lysine at the C-terminus. Subsequently, we cloned and overexpressed this protein in *Escherichia coli* [8]. This confirmed its identification as a RNase, since purified recombinant P2 could cleave RNA and was biochemically indistinguishable from the native enzyme. However, the understanding of its physiological role(s) is far from complete. The lack of significant sequence similarity to any known class of RNases and the absence of histidines — part of the active sites of most RNases — strongly suggest that it has independently evolved and developed its catalytic function.

The NMR structure of the wild type protein has recently been solved by Baumann et al. [9]. It consists of a triple-stranded anti-parallel β-sheet onto which an orthogonal double-stranded anti-parallel β-sheet is packed. In the present paper, structural characterization of the aromatic domain of the recombinant P2 has been performed by NMR and photo-CIDNP spectroscopies. In recent years the photo-CIDNP technique has been used to investigate a large number of proteins [10–13]. The photo-CIDNP effect arises from the nuclear spin polarization generated in a reversible photochemical reaction of a flavin dye with tyrosines, tryptophans and histidines on the protein surface. Our data show that the topological distribution of aromatic and hydrophobic residues occurring in this enzyme is that found in several RNA-binding proteins [14]; particularly, two residues, i.e. Phe$^{31}$, part of an aromatic cluster, and Trp$^{23}$, fully exposed to solvent, specifically interact with a flavin used as a model ligand. Thus, they are the best candidates for the interactions with RNA bases.

## 2. Materials and methods

The P2-encoding gene was chemically synthesized and expressed in *E. coli* and the purified protein found to be indistinguishable from the native enzyme on the basis of several biochemical criteria [8]. Spectra were collected in a temperature range of 300–340 K, pH 4.0, in both $H_2O$ and $^2H_2O$ and referenced to sodium trimethylsilyl[2,2,3,3-$^2$H4]sulfonate. NMR data were acquired with a Bruker AM-500 spectrometer equipped with an Aspect 3000 computer; P2 concentration was 2 mM. Standard pulse sequences were applied: 2D DQF COSY [15], Clean TOCSY [16], NOESY [17,18] and Scuba NOESY [19]. In all spectra the solvent suppression was achieved by presaturation of the water reso-

*Corresponding author. Fax: (39) (2) 266-3030.

*Abbreviations:* RNase, ribonuclease; RNP, ribonucleoprotein; photo-CIDNP, photo-chemically induced dynamic nuclear polarization; NMR, nuclear magnetic resonance, 2D DQF COSY, two-dimensional double quantum filtered correlated spectroscopy; Clean TOCSY, total correlation spectroscopy; Scuba NOESY, stimulated cross peaks under bleached alphas two-dimensional nuclear Overhauser effect spectroscopy.


*SSDI* 0014-5793(95)00940-X

nance during both relaxation and evolution times and the acquisition was carried out with 4096 data points in $t_2$ and 1024 $t_1$ increments, and a spectral width of 8064 Hz. Clean TOCSY spectra were collected using MLEV17 sequence for spin-locking with a mixing time of 60–100 ms. NOESY spectra were acquired with mixing times of 25, 50, 75, 100 and 150 ms. Before Fourier transformation, the data were zero-filled to 2048 points in the $t_1$ dimension and weighted with $\pi/3$ squared shifted sinebell in both dimensions. A baseline correction was performed in both dimensions using a polynomial function. Data were processed on a Bruker X-32 station using UXNMR program. $^1$H photo-CIDNP spectra were recorded on a Bruker AM-270 using a Coherent Innova 200 argon laser as the light source. A 300 ms light pulse (4 W, multiline) was used with a 50 ms delay before a 90° rf pulse to enhance cross-relaxation effects. Difference spectra were obtained by taking light and dark FIDs and subtracting the spectra after Fourier transformation. In the 2D photo-CIDNP [20] experiments, 32 'dark' and 32 'light' FIDs were recorded for each $t_1$ value. The first $t_1$ value of 20 ms was incremented with 0.6 ms steps, which corresponds to a spectral width of 801 Hz in the $\omega_1$ domain. The sample was irradiated during 50 ms with a 12 W light pulse or 300 ms with a 4 W light pulse, followed by a 50 ms delay. The difference spectra are presented in the absolute-value mode. Lumiflavin was from Sigma.

## 3. Results

Protein P2 contains five aromatic amino acid residues: one tryptophan ($Trp^{23}$), two phenylalanines ($Phe^5$ and $Phe^{31}$) and two tyrosines ($Tyr^7$ and $Tyr^{33}$). The assignments of the aromatic spin systems were obtained from 2D DQF-COSY, TOCSY, NOESY and photo-CIDNP experiments, using standard procedures. Sequence-specific assignments were obtained from sequential $\alpha CH_i$-$NH_{i+1}$, $\beta CH_i$-$NH_{i+1}$ and intraresidue $\beta$CH-2,6 aromatic NOE connectivities [21] (data not shown). NOE with $\beta$ protons and photo-CIDNP effects were used to distinguish between 2,6 and 3,5 proton resonances of $Tyr^7$ and $Tyr^{33}$. For $Phe^5$ it was not possible to distinguish the 2,6 and 3,5 resonances, because of overlapping. For $Trp^{23}$, NH1, H7 and H2 were determined from NOE spectra of the protein in a $H_2O$/$^2H_2O$ 9:1 solution. The chemical shifts of the aromatic residues are reported in Table 1.

In addition to the secondary chemical shifts, large shifts resulting from the presence of the five aromatic rings were observed to affect many residues (Table 1). In particular, the chemical shifts of all the aromatic protons, except $Tyr^7$, experienced significant upfield ring current shifts, compared to those expected for a random conformation; $Tyr^7$ exhibited a minor downfield shift.

In agreement with the structure proposed by Baumann et al. [9] for the wild type protein, the complete analysis of the NOEs (data not shown) indicated the presence of five strands of antiparallel $\beta$-sheets and two $\alpha$-helices. NOE effects within the set of aromatic protons were obtained from well resolved NOESY spectra (Table 2). They revealed the presence of an aromatic cluster consisting of four aromatic residues, namely $Phe^5$, $Tyr^7$, $Phe^{31}$ and $Tyr^{33}$, which interact with several aliphatic side chains. In particular the aromatic ring of $Phe^{31}$ is in close contact with the aromatic rings of $Phe^5$ and $Tyr^{33}$; $Val^{14}$ shows multiple contacts with $Phe^5$, $Tyr^{33}$ and $Phe^{31}$, while $Ile^{19}$ and $Ile^{29}$ interact with $Phe^{31}$ and/or $Tyr^{33}$; indeed, due to the close proximity with the aromatic rings, the side chains of these residues experience strong diamagnetic shifts (in particular $\Delta\delta$ = 0.3 ppm for $Val^3$ H$\gamma$,$\gamma'$; $\Delta\delta$ = 0.5 and 0.6 ppm for $Val^{14}$ H$\gamma$,$\gamma'$ and H$\beta$, respectively; $\Delta\delta$ = 0.3 for $Ile^{29}$ H$\gamma$ methyl; $\Delta\delta$ = 0.8 ppm for $Ile^{19}$ H$\delta$ methyl). The aromatic ring of $Trp^{23}$ appears completely exposed to solvent; its protons experience a strong upfield chemical shift, probably due to the interaction with four carbonyl groups, namely $Lys^{21}$, $Val^{22}$, $Ser^{30}$ and $Trp^{23}$ itself, which are in the range 3.7–4.6 Å from the aromatic protons.

By dissolving P2 in $^2H_2O$, a number of amide protons showed slow exchange rates (data not shown). In particular, 12 amide signals ($Val^{14}$, $Ile^{19}$, $Trp^{23}$, $Ile^{29}$, $Ser^{30}$, $Phe^{31}$, $Thr^{32}$, $Tyr^{33}$, $Gly^{43}$, $Val^{45}$, $Leu^{54}$ and $Leu^{55}$) remained after more than 40 h, and exchanged only at 320 K, suggesting a well-protected environment. Most of them correlate well with the expected pattern of hydrogen bonds in the five strands of $\beta$-sheets.

The photo-CIDNP method was used to investigate the access of a photoexcitable flavin dye to the aromatic cluster in order to determine the solvent exposure of each aromatic residue. Increasing amounts (in the range 16–80 $\mu$mol) of lumiflavin were added to a 2 mM solution of P2 in $^2H_2O$. An unusually large amount of flavin was necessary to observe a yellow fluorescent solution, suggesting the existence of specific interac-

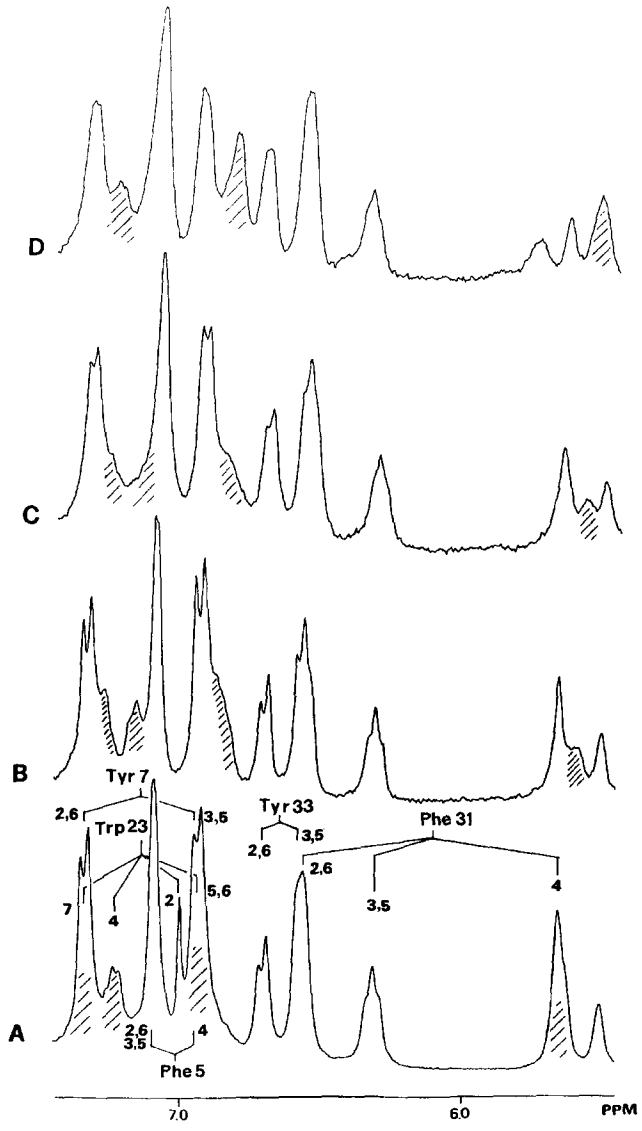


Fig. 1. Aromatic region of 270 MHz 1D NMR spectra of P2 in $^2H_2O$ solution pH 4.0, 300 K, upon addition of increasing amounts of flavin: (A) without dye, (B) with 48, (C) 64, and (D) 80 $\mu$mol of dye.

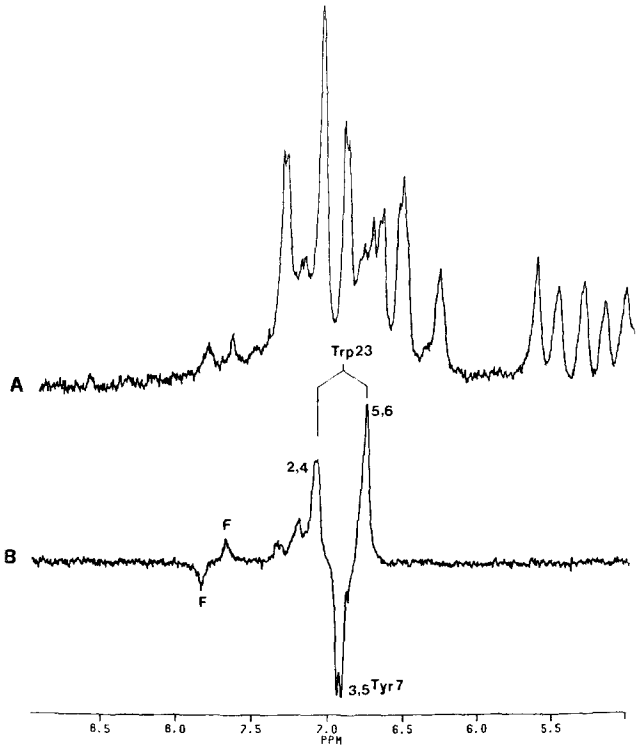


Fig. 2. (A) Aromatic region of a 270 MHz 1D NMR spectrum of P2 in $^2H_2O$ solution, pH 4.0, 300 K, in the presence of 75 $\mu$mol of flavin. (B) 270 MHz 1D photo-CIDNP difference spectrum obtained with 300 ms 4 W light pulse followed by a 50 ms delay before the 90° rf pulse; F denotes polarized flavin resonances.

tion(s) between the flavin dye and the protein. In keeping with hypothesis all signals of $Trp^{23}$ and $Phe^{31}$ were strongly upfield shifted (in particular, $\Delta\delta$ = 0.16 ppm for $Phe^{31}$ H4 and $\Delta\delta$ = 0.17 ppm for $Trp^{23}$ H5,6) and broadened, suggesting a specific interaction among flavin and the two aromatic residues (Fig. 1A–D). In agreement with this result, Baumann et al. [9] observed a change in the intrinsic tryptophan fluorescence upon interaction of the protein with polynucleotides. In contrast, $Phe^5$, $Tyr^7$ and $Tyr^{33}$ seemed not to be appreciably affected by the presence of flavin, either in the chemical shift or in the line-width.

The corresponding photo-CIDNP difference spectrum is shown in Fig. 2B. Only two out of the three polarizable residues, $Tyr^7$ and $Trp^{23}$ (but not $Tyr^{33}$), are strongly enhanced. The weak emissive resonance expected for $Tyr^7$ H2,6 [10] is not observed since it is cancelled by the absorptive $Trp^{23}$ H7 signal, which is cross-polarized by H6 (see 2D photo-CIDNP experiments below) during the 300 ms laser irradiation and the 50 ms preacquisition delay. The strong photo-CIDNP effect of $Tyr^7$ and $Trp^{23}$ indicates that the flavin dye used to generate spin polarization has full accessibility to the OH and N1 moieties, respectively, of these residues.

Fig. 3A and B show the aromatic region of 2D COSY photo-CIDNP spectra of P2 in $^2H_2O$ acquired with different irradiation times. In apparent contrast with the simplicity of the 1D spectrum, several cross-peaks are observed in the 2D spectra corresponding to additional photo-polarized residues. The longer irradiation time experiment (300 ms, Fig. 3A) shows that H3,5 of $Tyr^7$ clearly correlate with their H2,6, and H6 of $Trp^{23}$ with its H7. Due to the long irradiation pulse, back-polarization of these two systems is also observed. It is worth noting that the degeneracy of $Tyr^7$ H2,6 and $Trp^{23}$ H7 protons is abolished in the 2D experiment. The direct $Trp^{23}$ H4-H5 polarization is also observed together with its back-polarization; finally, a strong diagonal peak is observed for the directly polarized $Trp^{23}$ H2. A photo-CIDNP effect appears as well for $Tyr^{33}$ in the experiment with longer irradiation time (Fig. 3A) and this system is also present, but weaker, in the spectrum recorded with short irradiation time (Fig. 3B). No emissive signal was observed in the 1D photo-CIDNP spectrum for $Tyr^{33}$ H3,5, thus suggesting that the presence of this cross-peak in the 2D spectra is due to cross-polarization from $Tyr^7$, since NOEs were detected between $Tyr^7$ and $Tyr^{33}$. The intensities of $Tyr^{33}$ resonances appear enhaced by increasing the irradiation time (Fig. 3A).

Three additional diagonal peaks are observed for the $Phe^{31}$ aromatic protons (Fig. 3A), cross-polarized by the flavin which we have shown to specifically interact with $Phe^{31}$ and $Trp^{23}$. Several examples are reported of indirect polarization of residues in close contact with strongly polarized aromatic residues [22–24]. In particular, photo-CIDNP effects were observed in the presence of specific binding interactions between flavin and the protein [24,25]. In these examples the binding constant was not strong enough to prevent the radicals in the radical pair to separate ([10] and references therein) and photo-CIDNP effects could be observed. We therefore suggest that the same conditions apply to the P2–flavin interaction.

Table 1
$^1$H-NMR assignments and chemical shifts of aromatic protons of P2 in $^2H_2O$ solution, pH 4, 320 K. In parentheses deviations with respect to random coil chemical shift are reported

| | $Phe^5$ | $Tyr^7$ | $Trp^{23}$ | $Phe^{31}$ | $Tyr^{33}$ |
|---|---|---|---|---|---|
| 2,6 | 7.06 (0.31) | 7.31 (−0.14) | | 6.54 (0.83) | 6.68 (0.50 |
| 3.5 | 7.06 (0.31) | 6.93 (−0.03) | | 6.33 (1.04) | 6.54 (0.36) |
| 4 | 6.92 (0.45) | | | 5.73 (1.64) | |
| 2 | | | 6.99 (0.39) | | |
| 4 | | | 7.21 (0.52) | | |
| 5 | | | 6.90 (0.38) | | |
| 6 | | | 6.88 (0.40) | | |
| 7 | | | 7.31 (0.27) | | |
| αCH | 5.05 | 4.82 | 4.94 | 5.60 | 5.50 |
| NH | 8.58 | 8.91 | 9.26 | 7.54 | 8.56 |
| $\beta CH_2$ | 3.25 | 3.11 | 3.46 | 3.19 | 2.85 |
| $\beta' CH_2$ | 3.14 | 2.82 | 3.22 | 3.04 | 2.66 |

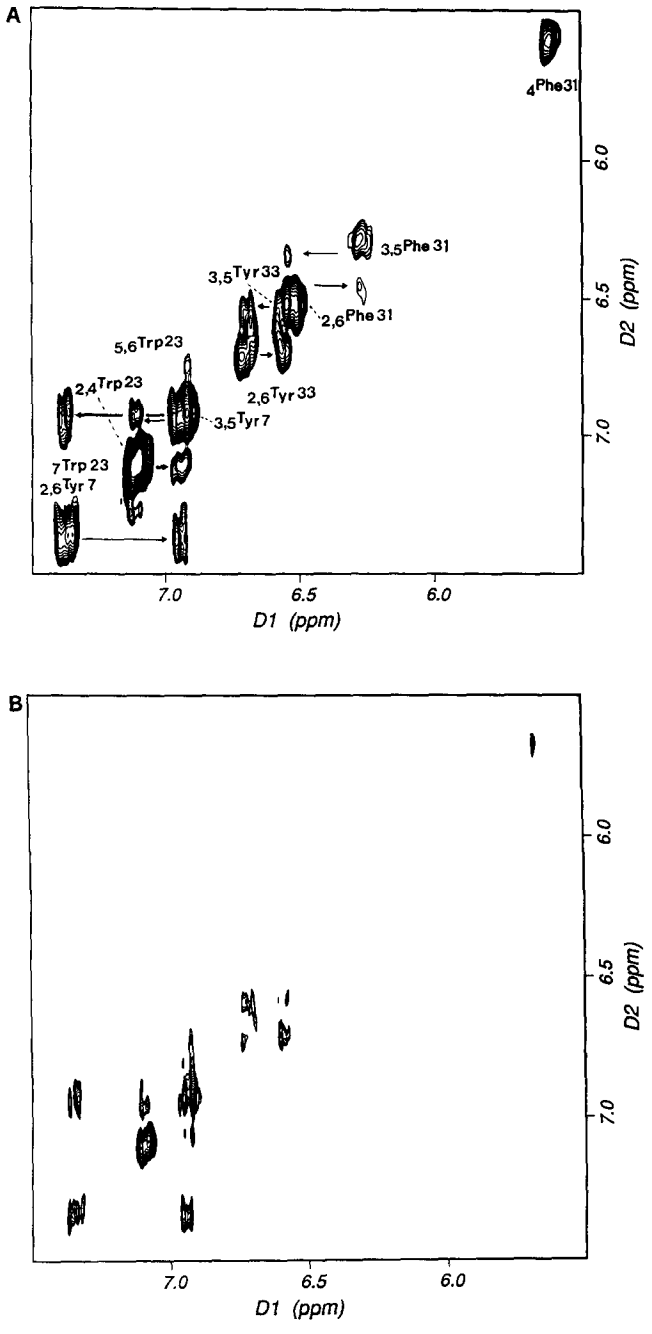


Fig. 3. 270 MHz 2D COSY photo-CIDNP spectra of P2 in $^2H_2O$ solution, pH 4.0, 300 K, in the presence of 64 $\mu$mol of flavin: (A) 300 ms 4 W light pulse, 50 ms delay; (B) 50 ms 12 W light pulse, 50 ms delay. Thick and thin arrows indicate direct and cross-polarization, respectively.

## 4. Discussion

The present work was mainly aimed at elucidating the presence in P2 of an aromatic cluster in view of its structural and functional relevance and at lightening the mode of interaction of RNase P2 with a photoexcitable flavin used as a model ligand. We found that four aromatic residues, namely Phe[5] and Tyr[7] in $\beta$1-strand, Phe[31] and Tyr[33] in $\beta$4 form an aromatic cluster, strongly interacting with the hydrophobic side chains of Val[14], Val[3], Ile[19] and Ile[29]. Trp[23] in $\beta$3 strand is fully exposed to solvent.

The same topological distribution of aromatic and hydrophobic residues is found in several RNA-binding proteins from eubacterial and eukaryotic sources, such as U1-A, U2-B, hnRNP, PABP, PPTB, nucleolin and others (reviewed in [14]). These proteins belong to a large family of molecules involved in RNA processing, in which a RNA recognition motif of about 80 amino acids represents the core of their RNA-binding domains [14,27,28]. Although the RNA-binding domains in these proteins have very low homology at the amino acid level, two consensus sequences, RNP1 and RNP2, have been identified. They are juxtaposed in adjacent $\beta$-strands and contain residues which are thought to be involved in nucleic acid binding; particularly, conserved aromatic side chains, critical for RNA binding, are clustered on the surface of the protein, close to the variable loop that determines recognition of specific RNA sequences [14,27,28]. In these proteins, involvement of the $\beta$-sheet region in RNA binding has been clearly established. In particular, the structural geometry of two exposed aromatic residues strongly suggests that nucleotide bases of RNA ligand might be involved in ring-stacking interactions with these aromatics at the protein-RNA interface.

Residues 22–27 (ValTrpArgValGlyLys) and 29–36 (IleSerPheThrTyrAspGluGly) of RNase P2 match RPN2 and RPN1 consensus sequences, respectively. Like in the case of the aforementioned RNA-binding proteins, P2 shows that two aromatics, namely Phe[31] and Trp[23], are accessible to the flavin dye and specifically interact with it, while, in contrast, Phe[5], Tyr[7] and Tyr[33] do not appear to be significantly affected. Photo-CIDNP experiments indicated that Tyr[7] and Trp[23] are exposed to the flavin dye, while Tyr[33] OH is buried. Indeed, Phe[31] is only partially exposed to solvent, but still appeared to be cross-

Table 2
Summary of the observed NOE effects from aromatic residues. NOE spectra were recorded in $^2H_2O$, pH 4, 300°K, $t_m$ = 150 ms

| amino acids | proton pair |
|---|---|
| F31–F5* | 4/2,6(3,5); 4 |
| F31–F5* | 3,5/2,6(3,5) 4 |
| F31 (Y33)*–Y33 | 2,6(3,5)/2,6;3,5 |
| F31–Y33 | 3,5/2,6;3,5 |
| F5*–Y7 | 2,6(3,5)/2,6;3,5 |
| F31–V14 | 4/$\gamma,\gamma'$ |
| F31–I19 | 4/$\delta$ |
| F31–T32 | 4/$\gamma$ |
| F31–F5 | 4/$\beta,\beta'$ |
| F31–Y33 | 3,5/$\beta,\beta'$ |
| F31–V14 | 3,5/$\beta,\beta,\gamma,\gamma'$ |
| F31–I19 | 3,5/$\gamma',\delta$ |
| F31–I29 | 3,5/$\gamma$ $CH_3$ |
| F31 (Y33)*–I19 | 2,6(3,5)/$\gamma'$,$\gamma CH_3,\delta$ |
| F31 (Y33)*–V22 | 2,6(3,5)/$\gamma,\gamma'$ |
| F31–I29 | 2,6/$\gamma CH_3$, $\beta$ |
| F5*–V14 | 2,6(3,5)/$\beta,\gamma,\gamma'$ |
| F5*–K12 | 2,6(3,5)/$\beta,\beta',\gamma$ |
| Y7–F31 | 3,5/$\beta$ |
| Y7–K12 | 2,6/$\gamma,\gamma'$ |
| W23–V25 | 2/$\gamma,\gamma'$ |
| W23–V22 | 2,4/$\gamma,\gamma'$ |
| W23–F31 | 4,5(6)/$\alpha$ |
| W23–T32 | 7,5(6)/$\gamma$ |
| Y33–F31 | 2,6/$\beta$ |
| Y33–V14 | 2,6/$\gamma,\gamma'$ |
| Y33–I19 | 2,6/$\alpha,\delta$ |

*NOE effects could not be unambigously identified, due to overlapping resonances in the two-dimensional spectrum.

polarized by the flavin, confirming the accessibility of this aromatic residue. Both $Trp^{23}$ and $Phe^{31}$ satisfy the exposure condition required by the RNA recognition motif, and the flavin seems to interact, probably through ring stacking interactions, with each of the two aromatic residues. This behaviour closely resembles the mode of interaction of other RNA-binding proteins in the base recognition process. On the other hand, it is well known that flavin can interact via ring stacking with aromatic residues such as tryptophans, tyrosines and phenylalanines. In particular, the non-covalently bound flavin cofactor in flavodoxins and in a $Tyr^{98}Trp$ mutant [29] are sandwiched between the aromatic in position 98, roughly parallel to it, and $Trp^{60}$ about 45° from being parallel [30,31].

Investigations made on the mutant $Phe^{31}Ala$ also supported the idea that $Phe^{31}$ plays a crucial role both in protein structure and function, since such mutation both dramatically destabilized the protein and substantially reduced its RNase activity (unpublished results).

Despite its lack of sequence similarity with other RNA-binding proteins, it is noteworthy that RNase P2 from *S. solfataricus* shares with these molecules the same structural motif, and possibly, the mode of binding, even though its size is significantly smaller than that of the RNA recognition motif from eubacterial and eukaryotic sources, i.e. 62 vs. 80 residues. These data confirm therefore that P2 has evolved independently its structure and mode of interaction with RNA.

*Acknowledgements:* This work was supported by grants from the Ministero dell'Università e della Ricerca Scientifica e Tecnologica (40% program) and from the Consiglio Nazionale delle Ricerche. The authors thank Fulvia Greco and Giulio Zannoni for skilful technical assistance in the NMR measurements and Lucia Zetta for helpful discussions.

## References

[1] Deutscher, M.P. (1988) Trends Biochem. Sci. 13, 136–139.
[2] Deutscher, M.P. (1993) J. Biol. Chem. 268, 13011–13014.
[3] Darr, S.C., Brown, J.W. and Pace, N.R. (1992) Trends Biochem. Sci. 17, 178–182.
[4] Fusi, P., Tedeschi, G., Aliverti, A., Ronchi, S., Tortora, P. and Guerritore, A. (1993) Eur. J. Biochem. 211, 305–310.
[5] Grote, M., Dijk, J. and Reinhardt, R. (1986) Biochim. Biophys. Acta 873, 405–413.
[6] Choli, T., Wittman-Liebold, B. and Reinhardt, R. (1988) J. Biol. Chem. 263, 7087–7093.
[7] Choli, T., Henning, P., Wittman-Liebold, B. and Reinhardt, R. (1988) Biochim. Biophys. Acta 950, 193–203.
[8] Fusi, P., Grisa, M., Mombelli, E., Consonni, R., Tortora, P. and Vanoni, M. (1995) Gene 154, 99–103.
[9] Baumann, H., Knapp, S., Lundbäck, T., Ladenstein, R. and Härd, T. (1994) Struct. Biol. 1, 808–819.
[10] Kaptein. R. (1978) in: NMR Spectroscopy in Molecular Biology (Pullman, B. ed.) pp. 211–229, D. Reidel, Dordrecht.
[11] Hore, P.J. and Broadhurst, R.W. (1993) Prog. NMR Spectrosc. 25, 345–402.
[12] Improta, S., Molinari, H., Pastore, A., Consonni, R. and Zetta, L. (1995) Eur. J. Biochem. 227, 78–86.
[13] Improta, S., Molinari, H., Pastore, A., Consonni, R. and Zetta, L. (1995) Eur. J. Biochem. 227, 87–96.
[14] Kenan, D.J., Query, C.C. and Keene, J.D. (1991) Trends Biochem. Sci. 16, 214–220.
[15] Piantini, U., Sorensen, O.W. and Ernst, R.R. (1982) J. Am. Chem. Soc. 104, 6800–6801.
[16] Griesinger, C., Otting. G., Wüthrich, K. and Ernst, R.R. (1988) J. Am. Chem. Soc. 114, 7870–7872.
[17] Jeener, J., Meier, B.H., Bachmann, P. and Ernst, R.R. (1979) J. Chem. Phys. 71, 4546–4553.
[18] Kumar, A., Ernst, R.R. and Wüthrich, K. (1980) Biochem. Biophys. Res. Commun. 28, 4914–4922.
[19] Brown, S.C., Weber, P.L. and Mueller, L. (1988) J. Magn. Reson. 77, 166–169.
[20] Stob, S., Scheek, R.M., Boelens, R., Dijkstra, K. and Kaptein, R. (1984) Faraday Disc. Chem. Soc. 78, 245–256.
[21] Wüthrich, (1986) NMR of Proteins and Nucleic Acids, Wiley, New York.
[22] Moonen, C.T.W., Hore, P.J., Müller, F., Kaptein, R. and Mayhew, S.G. (1982) FEBS Lett. 149, 141–149.
[23] Hore, P.J., Egmond, M.R., Edzes, H.T. and Kaptein, R. (1982) J. Magn. Reson. 49, 122–150.
[24] De Marco, A., Petros, A.M., Llinàs, M., Kaptein, R. and Boelens, R. (1989) Biochim. Biophys. Acta 994, 121–137.
[25] Moonen, C.T.W., Hore, P.J., Müller, F., Kaptein, R. and Mayhew, S.G. (1982) FEBS Lett. 149, 141–149.
[26] Redfield, C., Dobson, C.M., Scheek, R.M., Stob, S. and Kaptein, R. (1985) FEBS Lett. 185, 248–252.
[27] Hoffman, D., Query, C., Golden, B.L., White, S.W. and Keen, J.D. (1991) Proc. Natl. Acad. Sci. USA 88, 2495–2499.
[28] Burd, C.G. and Dreyfuss, G. (1994) Science 265, 615–621.
[29] Watt, W., Tulinsky, A., Swenson, R.P. and Watenpaugh, K.D. (1991) J. Mol. Biol. 218, 195–208.
[30] Watenpaugh, K.D., Sieker, L.C. and Jensen, L.H. (1973) Proc. Natl. Acad. Sci. USA 70, 3857–3860.
[31] Swenson, R.P. and Krey, G.D. (1994) Biochemistry 33, 8505–8514.

**Note:** After having submitted the manuscript to FEBS Letters, the authors found out in the literature a paper by Baumann et al. [9], concerning the solution structure of the wild form of the same protein described in the present paper.